

Low-temperature transport properties of *p*-type CoSb₃

D. T. Morelli

Physics Department, General Motors Research and Development Center, Warren, Michigan 48090

T. Caillat, J.-P. Fleurial, A. Borshchevsky, and J. Vandersande

Jet Propulsion Laboratory, California Institute of Technology, Pasadena, California 90210

B. Chen and C. Uher

Department of Physics, University of Michigan, Ann Arbor, Michigan 48109

(Received 27 October 1994)

Single crystals of the skutterudite CoSb₃ exhibit large hole mobilities (up to 3000 cm² V⁻¹ s⁻¹ at room temperature), intrinsic lattice thermal conductivity down to 10 K, and pronounced drag effects in the thermoelectric power. The dependence of the mobility and diffusion thermopower on hole density is consistent with recent band-structure calculations, which indicate that CoSb₃ possesses a highly nonparabolic valence-band structure.

I. INTRODUCTION

Skutterudite compounds have recently been identified as strong candidates for advanced thermoelectric materials.^{1,2} These compounds derive their name from the natural cubic mineral CoAs₃, the structure of which was investigated by Oftedal in 1928.³ The skutterudite family consists of compounds of the form AB₃, where *A* is Co, Ir, or Rh, and *B* is As, P, or Sb. In this structure, shown in Fig. 1, the pnictide atoms constitute four-membered rings located at the centers of cubes formed by the metal atoms.^{4,5} Very little is known about the physical properties of these materials. In a series of papers in the late 1950's and early 1960's,⁶⁻⁹ Dudkin and co-workers investigated the transport properties of CoSb₃ above room temperature. From the activated nature of the resistivity they concluded that this material was a semiconductor with a band gap of approximately 0.5 eV. Hulliger¹⁰ also concluded that skutterudites were semiconductors based on his observations of diamagnetism and large Seebeck coefficients. It should be mentioned that all of the above experiments were performed on pressed powders. Acker-

mann and Wold¹¹ prepared single crystals of Co skutterudites and found that while all three were diamagnetic, only CoP₃ exhibited an optical band gap; their samples of CoSb₃ and CoAs₃ displayed a metallic electrical resistivity below room temperature. Finally, Kliche and co-workers,¹²⁻¹⁵ based on far-infrared measurements, concluded that CoP₃, CoAs₃, CoSb₃, and RhSb₃ were semiconductors; on the other hand, they observed metallic conduction in RhSb₃ and a zero crossing in the Hall coefficient of CoAs₃, behavior which they suggested was extrinsic in origin.

The brief summary of the physical properties of skutterudites given above serves to show that our knowledge of these materials is at best sketchy and controversial in nature, in particular with regard to the question of semiconductivity in these compounds. This fact, together with the renewed interest in their thermoelectric properties, would be reason enough to undertake a detailed and systematic investigation of their transport properties. This situation, however, has been rendered even more thought provoking by the recent¹⁶ band-structure calculations for CoAs₃, CoSb₃, and IrSb₃ by Singh and Pickett (SP). These workers found that, in agreement with the earlier band-structure calculations of Jung, Whangbo, and Alvarez,¹⁷ a relatively large (~1 eV) gap forms around the Fermi level in these compounds, but that a single valence band crosses the gap, touching the conduction band in IrSb₃ and CoAs₃, and nearly doing so in CoSb₃. Thus SP concluded that these materials are actually zero- and narrow-gap semiconductors, with a highly nonparabolic band structure in the case of the antimonides. We feel that the combination of the recent strong interest in these materials, the controversial and incomplete nature of existing experimental data, and the band-structure predictions of SP, call for a detailed investigation of the low-temperature transport properties of skutterudites. We have chosen to begin with CoSb₃ because this compound is the easiest to fabricate in single-crystal form.

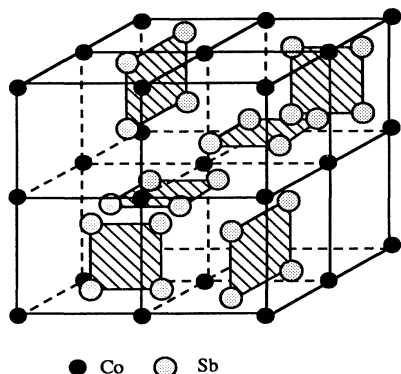


FIG. 1. The skutterudite structure.

II. EXPERIMENT

Starting constituents for the growth of our samples were Co (99.998% pure) and Sb (99.9999% pure). An impurity analysis of the cobalt detected only Al, Ca, Mg, and Ag, all at levels of less than 1 ppm. Single crystals were grown using the gradient freeze technique from melts with 93-at. % Sb in sealed quartz ampoules, the latter having been coated with graphite and provided with a pointed tip. A temperature gradient of approximately 50°C cm^{-1} was maintained at the growth interface. Typical ingots obtained after the growth were composed of two parts, the bottom part corresponding to the compound CoSb₃ and the upper part to the Sb-rich eutectic. Single-crystalline samples were obtained as indicated by Laue patterns. Selected samples were polished, and their microstructure examined, under an optical microscope. Microprobe analysis was also performed on the same samples to determine their composition. Finally, some samples were ground for x-ray-diffractometry analysis. These experiments showed that the samples were single phase with a lattice constant indicative of a Co:Sb ratio of 1:3. The density of all samples was measured by the immersion technique using toluene as the liquid. The measured densities were found to be approximately 99.5% of the theoretical density of 7.69 g cm^{-3} , confirming the stoichiometric ratio of 1:3. We have found, in agreement with Dudkin,⁷ that all unintentionally doped material is *p* type. Several samples were prepared with hole concentrations in the range 2.6×10^{17} – $4.1 \times 10^{18}\text{ cm}^{-3}$.

Thermopower, van der Pauw, and thermal conductivity measurements were carried out at room temperature on these samples at Jet Propulsion Laboratory as described earlier.¹⁸ Four of these samples, as shown in Table I, were large enough for the low-temperature measurements described in this paper. One of these, designated 52NB14, was not large enough to carry out low-temperature thermal conductivity and thermoelectric power measurements, but low-temperature galvanomagnetic data were obtained on this sample.

Thermal transport measurements were carried out by the four-probe steady-state technique which has been described in detail elsewhere.^{19,20} Samples were cut with a high-speed diamond saw in the shape of parallelepipeds with heat flow along the longest axis. Since the CoSb₃

structure is cubic, the lattice thermal conductivity, which as we will see is the predominant contribution, is essentially isotropic. Heat input to the sample was made via a metal film heater epoxied to the free end of the crystal. The temperature difference along the sample was measured with either Chromel-Constantan or AuFe-Chromel thermocouples above 20 K and with carbon glass thermometers at lower temperatures, and results differed by less than 5% in the overlap region. For Seebeck probes, we used either Pb or Cu wires, the absolute thermopower of each having been previously calibrated.^{21,22} In either case the absolute Seebeck coefficients of these probes do not exceed $1.5\ \mu\text{V K}^{-1}$ in the temperature range of interest.

Measurements of thermal conductivity κ and thermopower S were carried out in a closed-cycle helium refrigerator with a base temperature of 11 K. In order to extend data on one sample (71NB13) to lower temperature, this sample was remounted in a liquid-helium cryostat. We estimate the absolute error in our measurements of κ and S as 10%, which arises from the error in measuring the geometrical factor of these small samples.

The electrical resistivity, carrier concentration, and mobility were measured on disks of material using the van der Pauw technique with sample currents in the range 1–30 mA. Care was taken to insure that no heating of the samples occurred during the course of a measurement. The hole concentration p was determined from the Hall coefficient R_H (which was independent of field to within 5% up to 6 T) using $R_H = 1/pe$, i.e., assuming a scattering factor equal to 1 and a single-carrier model. On one sample (71NB13) Hall measurement was repeated on the parallelepiped using the standard Hall geometry, and the results agreed with those using the van der Pauw technique to within 10%. The hole mobility ν was determined from the zero-field resistivity ρ and the carrier concentration p using $\rho = 1/(pe\nu)$.

Finally, magnetic-susceptibility measurements were carried out between 4 and 300 K using a Quantum Design superconducting quantum interference device (SQUID) magnetometer. The samples were placed inside of a polyethylene capsule and straw, and the background susceptibility was independently measured and accounted for. Due to the small susceptibility of the samples, we estimate an error in this measurement of approximately 10%.

III. RESULTS

A. Hole concentration and hole mobility

Table I indicates the room-temperature hole concentration, hole mobility, thermal conductivity, Seebeck coefficient, and magnetic susceptibility of four nominally undoped samples of *p*-CoSb₃. The large hole mobility is consistent with the predominantly covalent bonding in this compound. For comparison, Slack and Tsoukala² found a mobility of $1320\text{ cm}^2\text{ V}^{-1}\text{ s}^{-1}$ on an IrSb₃ sample with a hole concentration of $1.1 \times 10^{19}\text{ cm}^{-3}$. The thermal conductivity is fairly small due to the large atom masses and complex unit cell. This combination of large

TABLE I. Parameters of *p*-type CoSb₃ crystals. p is the hole concentration (cm^{-3}) at 300 K; ν is the hole mobility ($\text{cm}^2\text{ V}^{-1}\text{ s}^{-1}$) at 300 K; κ is the thermal conductivity ($\text{W cm}^{-1}\text{ K}^{-1}$) at 300 K; S is the thermoelectric power ($\mu\text{V K}^{-1}$) at 300 K; χ is the magnetic susceptibility ($10^{-5}\text{ emu G}^{-1}\text{ mol}^{-1}$) at 300 K; and β_2 is the low-temperature saturation value of the mobility ($\text{cm}^2\text{ V}^{-1}\text{ s}^{-1}$).

Sample	p	ν	κ	S	χ	β_2
52NB14 ○	2.6×10^{17}	2775			−4.1	9800
71NB13 ●	1.2×10^{18}	2445	0.115	216	−7.7	7300
2NB14 □	3.6×10^{18}	2175	0.129	167	−8.7	6700
1NB14 ▲	4.1×10^{18}	1746	0.102	130	−8.9	5600

carrier mobility and fairly small thermal conductivity is why these materials are promising as thermoelectrics. Figures 2(a) and 2(b) display the temperature dependence of the hole concentration and mobility, respectively, of these four samples. The hole concentration decreases weakly down to 4 K. Between 300 and 100 K the mobility increases with decreasing temperature approximately as $T^{-1.5}$, before saturating at a value at low temperature which scales inversely with the hole concentration. For

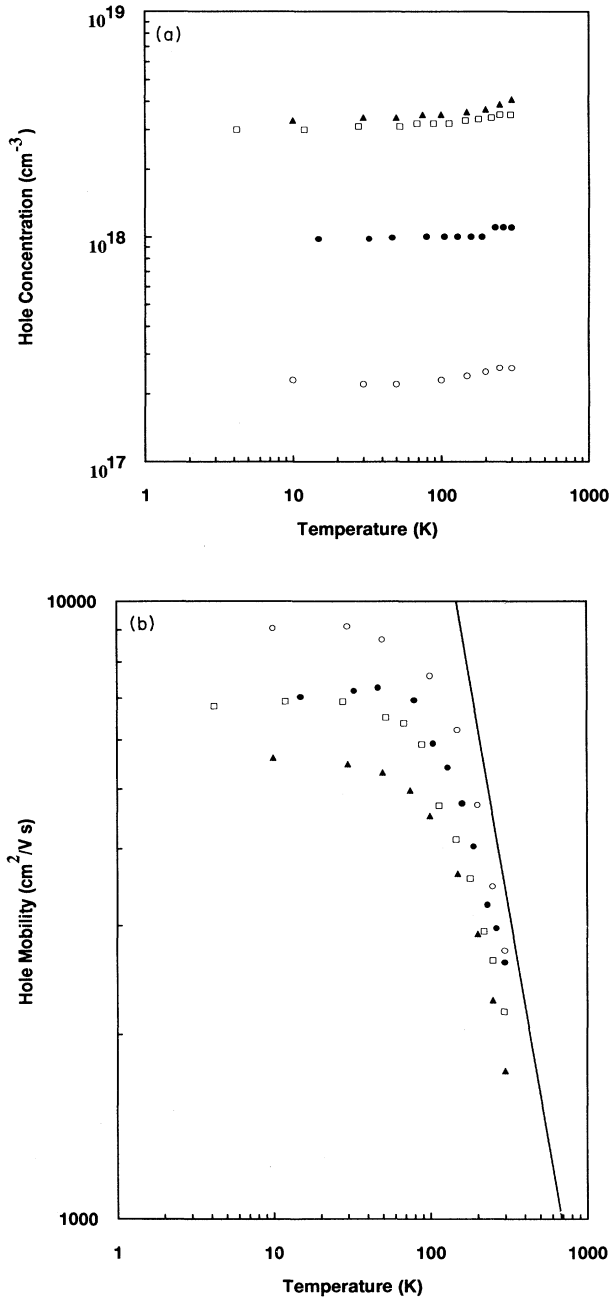


FIG. 2. (a) Hole concentration and (b) hole mobility of four samples of *p*-type CoSb_3 ; the solid line in (b) shows the $T^{-1.5}$ dependence. The sample designation is given in Table I.

the lowest doped sample, the mobility reaches nearly $10^4 \text{ cm}^2 \text{ V}^{-1} \text{ s}^{-1}$ at 4 K.

B. Thermal conductivity

Figure 3 shows the thermal conductivity as a function of temperature. The dashed line represents the high-temperature results of Slack and Tsoukala for IrSb_3 . From the measured value of the electrical resistivity and the Wiedemann-Franz law, we estimate that the electronic contribution to κ for our CoSb_3 samples is less than 10% for all samples and temperatures. Thus the measured thermal conductivity shown in Fig. 3 is essentially the lattice thermal conductivity. The very steep rise in κ with decreasing temperature is characteristic of the predominance of phonon-phonon umklapp scattering and is a testament to the purity of the samples. In fact, very few materials actually show the exponential increase in conductivity with decreasing temperature as predicted by Peierls when U processes are the only resistive scattering process. This is because even in the purest crystals, the presence of isotopes of different mass provides a source of point-defect scattering which causes the conductivity to rise much more slowly than exponentially.²³ Interestingly, it is to be noted that Co has only a single isotope and Sb only two with a relative mass difference of less than 2% (in fact, Co, Rh, P, and As are *all* monoisotopic, and pure single crystals of skutterudites made up of combinations of these elements should all exhibit exponentially rising thermal conductivity at low temperature). Thus point-defect scattering due to isotopic mass fluctuations

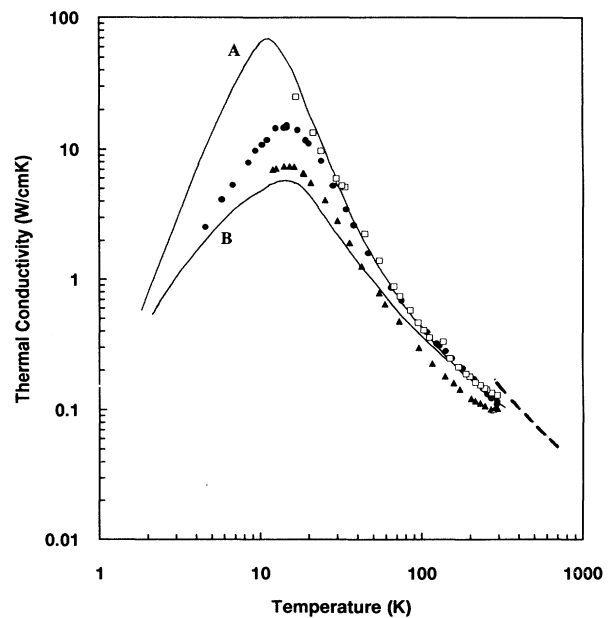


FIG. 3. Thermal conductivity of three samples of *p*-type CoSb_3 . The sample designation is given in Table I. Curve *A* is a fit to the Debye model assuming Umklapp and boundary scattering of phonons; curve *B* includes the effect of $1 \times 10^{18} \text{ cm}^{-3}$ vacancies. The dashed line represents high-temperature results on IrSb_3 (Ref. 2).

is essentially absent in these materials, and apparently the concentration of other types of defects and impurities is very small. What is surprising is that the rapid rise in thermal conductivity occurs despite the fact that these materials are electrically conducting. We are aware of no previous such observation on an electrically conducting material except the semimetal bismuth, another element with only a single isotope. While there is some sample dependence of κ near the peak in CoSb₃, it does not scale with hole concentration.

C. Seebeck coefficient

Figure 4 exhibits the thermoelectric power of our three samples of CoSb₃. The magnitude of the thermopower scales inversely with hole concentration and decreases roughly linearly with temperature down to 100 K, indicative of the predominance of hole diffusion thermopower. Below 100 K $S(T)$ rises dramatically and develops a peak at approximately the same temperature as the peak in the thermal conductivity. This coincidence of maxima in $S(T)$ and $\kappa(T)$ is evidence that this feature in the Seebeck coefficient is a strong phonon drag effect (we eliminate a Kondo phenomenon as the source of this peak, since there is no evidence of magnetic impurities in these samples; see Sec. III D).

D. Magnetic susceptibility

Figure 5 exhibits the magnetic susceptibility of *p*-type CoSb₃ after correcting for the background susceptibility of the sample holder. We see that the susceptibility is small, diamagnetic, and essentially temperature independent, in agreement with previous studies.^{10,24} The solid line indicates the ion core contribution to $\chi(T)$ estimated from the atomic susceptibilities of the constituents.²⁵ Due to the inaccuracy of estimating this latter contribution, it is difficult to say anything quantitative about the magnetic susceptibility; we simply note that there appears to be a small diamagnetic and essentially

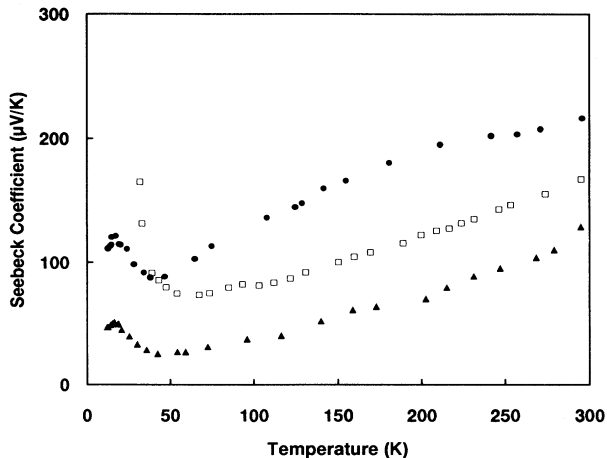


FIG. 4. Thermoelectric power of three samples of CoSb₃; the sample designation is indicated in Table I.

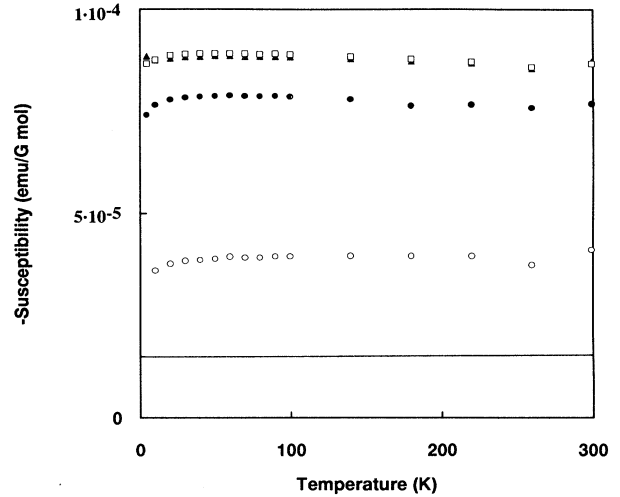


FIG. 5. Magnetic susceptibility of four samples of *p*-type CoSb₃, with the sample designation given in Table I. The solid line indicates the estimated ion core contribution.

temperature-independent contribution from the carriers, and leave this subject without further analysis.

IV. DISCUSSION

As indicated above, the temperature dependence of the hole mobility is suggestive of a combination of scattering by phonons at high temperature (above 100 K) and neutral impurities below 100 K. In fact the data in Fig. 2(b) can be fit using the empirical relation

$$\nu^{-1} = \nu_p^{-1} + \nu_{ni}^{-1} \quad (1)$$

with the phonon-limited mobility $\nu_p = \beta_1 T^{-1.5}$ and the neutral-impurity-limited mobility $\nu_{ni} = \beta_2$. The best fit occurs for $\beta_1 = 1.8 \times 10^7 \text{ cm}^2 \text{ V}^{-1} \text{ s}^{-1} \text{ K}^{3/2}$ and for the values of β_2 given in Table I. The absence of ionized impurity scattering (as evidenced by the lack of a $T^{3/2}$ dependence of mobility at lower temperatures) is quite surprising given the relatively large hole concentration in these materials. One might surmise that this is due to a strong screening effect. While the dielectric constant of CoSb₃ is indeed fairly large ($\epsilon_\infty \approx 25$; Ref. 26), it is roughly the same as that in InSb (~ 18), a material in which ionized impurity scattering is known to be quite strong, and it is much smaller than in PbTe (~ 2000 at low temperature), the prototypical material in which ionized impurity scattering is suppressed due to screening. On the other hand, if the holes were intrinsic and excited across a gap of 50 meV (such as that suggested by the SP band-structure calculation), their intrinsic density at 300 K would be about 10^{17} cm^{-3} , thus these samples are mostly extrinsic in the temperature range studied here. The small variation in hole concentration with temperature in the two most lightly doped samples is in fact consistent with a gap on the order of 100 meV. Given the lack of ionized impurity scattering, the origin of the extrinsic carriers in this material is an open question, the answer

to which awaits further investigation.

One of the predictions of the SP band-structure model is that when the constant scattering time approximation holds, i.e., when the scattering of holes is energy independent, the hole mobility, which is normally independent of doping level under these conditions, will vary as $p^{-1/3}$. Now the scattering time is energy independent for scattering from neutral impurities, which is just the case in CoSb₃ at low temperatures. Thus we can compare directly the low-temperature saturation value of the mobility with the predicted behavior according to SP. Figure 6 shows the low-temperature hole mobility as a function of hole concentration. Indeed, the $p^{-1/3}$ law is reasonably closely followed for this material, in good agreement with the SP band-structure model.

We turn now to a discussion of the thermal conductivity and thermoelectric power. As discussed above, the thermal conductivity is due almost entirely to the lattice, and we can attempt a fit to the data using the Debye model²⁷ and assuming only phonon-phonon umklapp scattering and boundary scattering. The frequency ω and temperature dependence of the U -process scattering rate τ_{pp}^{-1} in principle can be determined if one has knowledge of the phonon dispersion curves, for instance using the procedure of Han and Klemens.²⁸ Unfortunately no information is available with regard to the phonon-dispersion relations in CoSb₃. Therefore, we shall make use of the empirical relation $\tau_{pp}^{-1} \sim \omega^2 T \exp(-\theta/3T)$, where θ is the Debye temperature. This form for the umklapp scattering rate has been used with success for a variety of covalently bonded semiconductors, including Si and Ge (Ref. 29) and diamond.³⁰ Berman²⁷ has shown that, at least for the temperature range considered here, the particular values chosen for the frequency and temperature prefactors in this equation are somewhat arbitrary, since

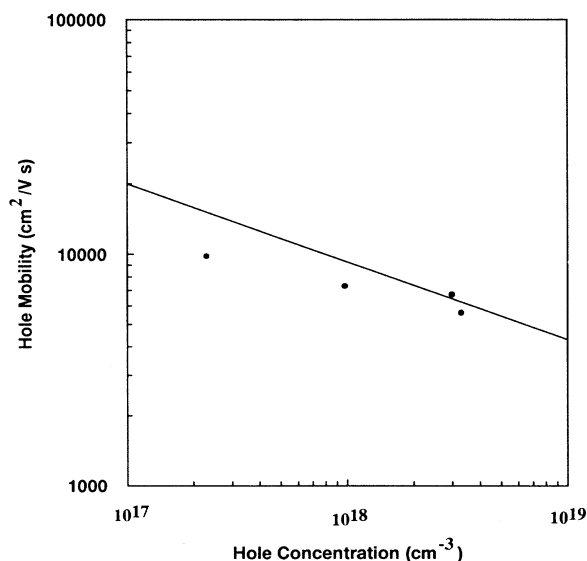


FIG. 6. Low-temperature saturation value of the hole mobility as a function of hole concentration for p -CoSb₃. The solid line is the $\nu \sim p^{-1/3}$ behavior.

the temperature dependence is determined largely by the exponential; we have chosen the above form simply on the basis that it has been used successfully for the aforementioned materials over very wide temperature ranges. For the boundary scattering rate we take $\tau_b^{-1} = v/L$, where v is an average phonon velocity and L is a characteristic sample dimension. The Debye temperature and phonon velocity are related to each other by²

$$\theta = 297.72(v/\delta), \quad (2)$$

where δ^3 is the average volume occupied by an atom. Curve *A* in Fig. 3 is the best fit to the data of sample 2NB14 using $L = 1$ mm and yields $\theta = 287$ K and $v = 2700$ m s⁻¹. These values are in good agreement with the values $\theta = 306$ K and $v = 2930$ m s⁻¹ determined from our ultrasonic measurements, and are to be compared with values of $\theta = 308$ K, $v_{\text{long}} = 4675$ m s⁻¹, and $v_{\text{trans}} = 2717$ m s⁻¹ for IrSb₃.² Thus the measured lattice thermal conductivity of CoSb₃ above the maximum is nearly what one expects given the crystal structure and elastic constants of this compound. If we were to assume that the holes observed in the electrical transport originated from charged vacancies, one would expect that the thermal conductivity would be reduced due to phonon-vacancy point-defect scattering. For a vacancy concentration of 1×10^{18} cm⁻³ (sufficient to produce 3×10^{18} cm⁻³ holes, each vacancy providing three holes⁷), the resultant thermal conductivity would be that indicated by curve *B* in Fig. 3, which exhibits a much slower rise and smaller peak value than that observed. This curve was derived using the vacancy-phonon-scattering rate of Ratsifaritana and Klemens,³¹ which takes into account both the mass and elastic constant differences due to the presence of the vacancy. The acceptor impurity which would produce the least amount of phonon scattering is Sn substituting for Sb; in this case the mass difference is only 3%, and Sn impurities at a concentration of 3×10^{18} cm⁻³ would produce, assuming no strain effect, practically no phonon scattering. However, trace impurity analysis reveals a Sn concentration at least two orders of magnitude smaller than necessary to produce the observed hole concentrations, and in addition such an argument cannot explain the difference in thermal conductivity at the peak between samples 2NB14 and 1NB14. Taken together, these observations again stress the inexplicable origin of the holes in this material. Finally, it is possible that the thermal conductivity of sample 1NB14 is limited by other types of defects, such as dislocations, but we have not undertaken a detailed study along these lines.

Another point to be noted is that the phonon mean free path at low temperatures takes on a very large value. This very large phonon mean free path at low temperatures manifests itself in the occurrence of phonon drag thermopower in this material in this temperature range. From our measured values of thermal conductivity and mobility it is possible to make a rough estimate of the magnitude of the phonon drag component S_{pd} of the thermopower. We have³²

$$S_{pd} = (k_B/e)(m^*v/k_B T)(L_p/\tau_{hp}). \quad (3)$$

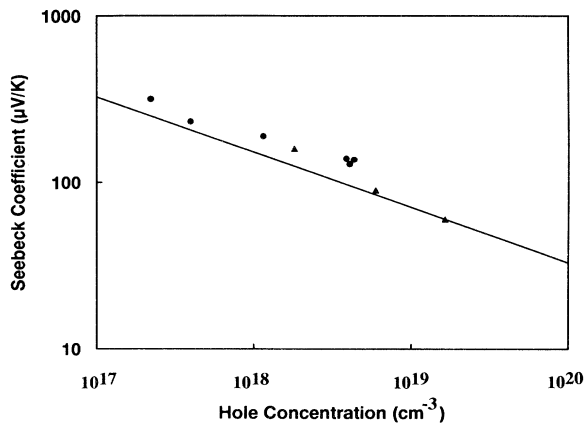


FIG. 7. Room-temperature thermoelectric power as a function of hole concentration in *p*-CoSb₃. Sample designation: ●, this work; ▲, Ref. 9. The solid line is the relation predicted by Eq. (4) for CoSb₃.

In this expression, $m^* \approx 0.1m_0$ is the hole effective mass,¹⁸ L_p the phonon mean free path, and τ_{hp} the hole-phonon scattering time. For $T=10$ K, we estimate $L_p \approx 0.1$ mm. The hole-phonon scattering time can be estimated from the phonon-limited mobility determined from the fit to our experimental mobility as given above: $\tau_{hp} = m^* v_p / e = m^* \beta_1 T^{-1.5} / e \approx 3 \times 10^{-11}$ s at this temperature. Thus from Eq. (3) at 10 K we find $S_{pd} \approx 300$ $\mu\text{V K}^{-1}$, in reasonable agreement with the observed values, given the very approximate nature of the scattering parameters.

Finally, we wish to compare the room-temperature thermoelectric power of our samples with that predicted by the SP band-structure model. In this model, the thermoelectric power is predicted to be

$$S = (2\pi k_B^2 T / 3e\alpha)(\pi/3p)^{1/3}, \quad (4)$$

where $\alpha = -3.1$ eV \AA is the slope of the linear dispersing band as calculated by SP. This expression has a different doping dependence than the normal parabolic band, for

which $S \sim p^{-2/3}$. Note that Eq. (4) contains no adjustable parameters, the thermopower depending only on the slope of the band, which is fixed by the band-structure calculation, and the measured hole concentration. Figure 7 shows the room-temperature thermoelectric power (where the phonon drag effect is negligible) versus carrier concentration for a variety of *p*-type CoSb₃ samples, including three Sn-doped samples measured by Zobrina and Dudkin.⁹ The solid line is the predicted value of Eq. (4) for CoSb₃, and the agreement is quite remarkable, especially in light of the fact that there are no adjustable parameters. SP also found that the one sample of Slack and Tsoukala² was consistent with their calculation. These findings thus lend strong support to the SP band-structure model of antimonide skutterudites.

V. SUMMARY

We have performed a detailed set of low-temperature transport measurements on CoSb₃ in order to clarify the nature of transport in this skutterudite and to compare the results with the recent band-structure model of Singh and Pickett.¹⁶ High-quality single crystals exhibit large hole mobilities, intrinsic lattice thermal conductivity down to 10 K, and pronounced phonon drag effects in the thermoelectric power. A comparison of the results with the predicted band structure seems to lend support to the picture that these skutterudites possess a highly nonparabolic valence band. On the other hand, based on the absence of ionized impurity scattering and the observation of an exponentially rising thermal conductivity at low temperature, the origin of the highly mobile holes in this material remains a mystery. We are planning further measurements of the low-temperature transport properties of both *p*- and *n*-type samples in order to further elucidate their behavior.

ACKNOWLEDGMENTS

The authors would like to acknowledge useful discussions with Dr. J. Herbst, Dr. J. Heremans, Dr. G. Meisner, Dr. D. Singh, and Dr. G. Slack.

¹T. Caillat, A. Borshchevsky, and J.-P. Fleurial, in *Proceedings of the XIth International Conference on Thermoelectrics, University of Texas at Arlington, 1992*, edited by K. R. Rao (University of Texas at Arlington Press, Arlington, 1993), p. 98.
²G. A. Slack and V. G. Tsoukala, *J. Appl. Phys.* **76**, 1665 (1994).
³I. Ofteidal, *Z. Kristallogr.* **66**, 517 (1928).
⁴A. Kjekshus and T. Rakke, *Acta Chem. Scand. A* **28**, 99 (1974).
⁵S. Rundquist and N.-O. Ersson, *Ark. Kemi* **30**, 103 (1968).
⁶L. D. Dudkin and N. Kh. Abrikosov, *Sov. J. Inorg. Chem.* **2**, 212 (1957).
⁷L. D. Dudkin, *Zh. Tekh. Fiz.* **28**, 240 (1958) [*Sov. Phys. Tech. Phys.* **3**, 216 (1958)].
⁸L. D. Dudkin and N. Kh. Abrikosov, *Fiz. Tverd. Tela (Leningrad)* **1**, 142 (1959) [*Sov. Phys. Solid State* **1**, 126 (1959)].

⁹B. N. Zobrina and L. D. Dudkin, *Fiz. Tverd. Tela (Leningrad)* **1**, 1821 (1959) [*Sov. Phys. Solid State* **1**, 1688 (1960)].
¹⁰F. von Hulliger, *Helv. Phys. Acta* **34**, 783 (1961).
¹¹J. Ackermann and A. Wold, *J. Phys. Chem. Solids* **38**, 1013 (1977).
¹²H. D. Lutz and G. Kliche, *Phys. Status Solidi B* **112**, 549 (1982).
¹³G. Kliche and W. Bauhofer, *Mater. Res. Bull.* **22**, 551 (1987).
¹⁴G. Kliche and W. Bauhofer, *J. Phys. Chem. Solids* **49**, 267 (1988).
¹⁵G. Kliche, *Sol. State Commun.* **80**, 73 (1991).
¹⁶D. J. Singh and W. E. Pickett, *Phys. Rev. B* **50**, 11 235 (1994).
¹⁷D. Jung, M.-H. Whangbo, and S. Alvarez, *Inorg. Chem.* **29**, 2252 (1990).

- ¹⁸T. Caillat, A. Borshchevsky, and J.-P. Fleurial, in *Proceedings of the XIII International Conference on Thermoelectrics*, edited by B. Mathiprakasam (AIP, New York, in press).
- ¹⁹D. T. Morelli, *Phys. Rev. B* **44**, 5453 (1991).
- ²⁰D. T. Morelli and C. Uher, *Phys. Rev. B* **28**, 4242 (1983).
- ²¹R. B. Roberts, *Philos. Mag.* **36**, 91 (1977).
- ²²C. Uher, *J. Appl. Phys.* **62**, 4636 (1987).
- ²³G. A. Slack, *Phys. Rev.* **105**, 829 (1957).
- ²⁴C. M. Pleass and R. D. Heyding, *Can. J. Chem.* **40**, 590 (1962).
- ²⁵W. Klemm, in *Atomic and Molecular Physics. Atoms and Ions*, edited by A. Eucken, Landolt-Börnstein, Vol. I, Pt. 1 (Springer-Verlag, Berlin, 1950), p. 398.
- ²⁶G. Kliche and H. D. Lutz, *Infrared Phys.* **24**, 171 (1984).
- ²⁷R. Berman, *Thermal Conduction in Solids* (Clarendon, Oxford, 1976), p. 23.
- ²⁸Y.-J. Han and P. G. Klemens, *Phys. Rev. B* **48**, 6033 (1993).
- ²⁹C. J. Glassbrenner and G. A. Slack, *Phys. Rev.* **134**, A1058 (1964).
- ³⁰D. G. Onn, A. Witek, Y. Z. Qiu, T. R. Antohony, and W. F. Banholzer, *Phys. Rev. Lett.* **68**, 2806 (1992).
- ³¹C. A. Ratsifaritana and P. G. Klemens, *Int. J. Thermophys.* **8**, 737 (1987).
- ³²J. M. Ziman, *Electrons and Phonons* (Clarendon, Oxford, 1960), p. 449.